DEMODULATED SYNCHROSQUEEZING S-TRANSFORM AND ITS APPLICATION AND ECONOMIC VALUE IN SEISMIC DATA ANALYSIS

JUN ZHOU [1], LIEJUN LI [2], QINGNAN HE[1], WEI LIU [3] and HONGZHI MA[1]

[1]*Nanchang Institute of Science and Technology, Gezaoshan Road 998, Honggutan District, Nanchang 330108, P.R. China. 15304690053@163.com*
[2]*Nanchang Normal College of Applied Technology, Mingyueshan Road 1599 Honggutan District, Nanchang 330108, P.R. China.*
[3]*College of Mechanical and Electrical Engineering, Beijing University of Chemical Technology, North Third Ring Ring 15, Chaoyang District, Beijing 100029, P.R. China. liuwei_upc@126.com*

(Received January 20, 2023; accepted April 9, 2023)

ABSTRACT

Zhou, J., Li, L.J., He, Q.G., Liu, W. and Ma, H.Z., 2023. Demodulated synchrosqueezing S-transform and its application and economic value in seismic data analysis. *Journal of Seismic Exploration*, 32: 229-242.

The synchrosqueezing transforms based on short-time Fourier transform (FSST) and wavelet transform (SSWT) have been widely used in the analysis of non-stationary signals. In the light of the superiority of S-transform (ST) over short-time Fourier transform (STFT) and wavelet transform (WT) in time-frequency representation (TFR), we propose a novel time-frequency analysis method, termed as demodulate synchrosqueezing S-transform (DSSST), which achieves a highly energy-concentrated TFR by making full use of two operations including demodulation technique and ST-based synchrosqueezing transform (SSST). The formulas for the DSSST and its inverse transform are derived. Synthetic example shows that the DSSST has higher time-frequency resolution compared with the standard ST and SSST. Then we apply the DSSST to perform the spectral decomposition on a real field data including gas-filled sand. The results demonstrate that the DSSST can be utilized to well characterize the spectral anomalies related to hydrocarbon reservoir, which renders that this new approach is promising for seismic data analysis.

KEY WORDS: time-frequency representation. S-transform, synchrosqueezing transform, demodulate synchrosqueezing S-transform, hydrocarbon detection.

0963-0651/23/$5.00

INTRODUCTION

Time-frequency analysis (TFA) has been successfully applied in seismic data analysis over the past few decades, which decomposes 1D seismic signal into 2D time-frequency map in order to characterize the time-varying frequency response of seismic signal that reflects the subsurface reservoir (Castagna et al., 2003; Liu and Fomel, 2013; Chen et al., 2014). The common TFA techniques include the short-time Fourier transform (STFT) (Allen, 1977), wavelet transform (WT) (Sinh et al., 2005) and the S-transform (ST) (Stockwell et al., 1996). However, the time-frequency energy based on such transforms always spreads over a ribbon in the time-frequency spectrogram due to the Heisenberg uncertainty principle or the selection of window. Consequently, the inappropriate spectral anomalies often appear on the time-frequency map, which may lead to some mistakes on seismic interpretation based on spectral decomposition results. One of the solutions to this problem is to improve the time-frequency resolution of spectral decomposition.

Auger and Flandrin (1995) developed the reassignment method (RM) to enhance the resolution of a TFR by the aid of transferring the time-frequency coefficients from the original position to the center of gravity of signal's energy distribution along the time and frequency axes. Unfortunately, the RM does not allow for signal reconstruction. Synchrosqueezing transform (SST) that was first introduced by Daubechies et al. (2011) based on WT serves as an alternative to the empirical mode decomposition (EMD), which has greatly improved the readability of a TFR by means of reassigning the time-frequency coefficients in the frequency direction (Herrera et al., 2014). In addition, the SST not only has a rigorous theoretical foundation, but also has the inverse transform. Meanwhile, Thakur and Wu (2011) further extended the idea of synchrosqueezing to the STFT, and put forward the STFT-based SST (FSST) to retrieve the ideal TFR. Inspired by the SST and FSST, many new 'synchrosqueezing' transforms are emerging. For instance, Yang (2015) developed the synchrosqueezing wave packet transforms (SSWPT) for 1D general mode decomposition. Huang et al. (2016) proposed a synchrosqueezing S-transform (SSST) that is achieved with the help of synchrosqueezing the spectrum of the ST to detect frequency spectral anomalies correlated with the gas hydrate and free-gas accumulations. Wang et al. (2018) replaced the frequency-dependent Gaussian window in the standard S-transform by a parameterized function that is composed of three parameters, and put forward the synchrosqueezing generalized S-transform (SSGST) for seismic time-frequency analysis. Liu et al. (2019) proposed the self-adaptive generalized S-transform (SAGST) to extract information from seismic data by setting the parameter of the generalized S-transform (GST) adaptively using the instantaneous frequency of seismic traces. However, it is noteworthy that a weak frequency modulation hypothesis is made on the modes constituting the signal for the above methods. In other words, such approaches are unable to handle the signals with strongly varying instantaneous frequency well.

Compared with the STFT and WT, the ST has the obvious advantages in time-frequency characterization and phase retaining of signals. In this paper, we present a novel TFA method that we refer to as the demodulate synchrosqueezing S-transform (DSSST), in which the demodulation and synchrosqueezing techniques are utilized to estimate the instantaneous frequency. Then the DSSST is employed to enhance the time-frequency resolution of spectral decomposition of seismic signals. The structure of this paper is as follows. We first describe the basic principles of the ST and SSST, and then derive formulas for the DSSST and the signal reconstruction by its inverse transform. Next, a synthetic example illustrates the superior energy-concentration of DSSST in the time frequency map by comparing with the standard ST and SSST. Finally, we apply the DSSST to real field data in order to further demonstrate the potential of DSSST in hydrocarbon-saturated reservoir identification with high precision.

PRINCIPLES

S-transform

A signal s is defined as follows:

$$s(t) = A(t)e^{i2\pi\varphi(t)} \quad , \tag{1}$$

where $A(t)$ and $\varphi(t)$ denote the instantaneous amplitude and phase, respectively.

The S-transform of signal *s* is represented as:

$$ST_s = \frac{|f|}{\sqrt{2\pi} f_0 T}\int_{-\infty}^{+\infty} s(\tau) e^{-\left(\frac{f^2(t-\tau)^2}{2(f_0 T)^2} + jf\tau\right)} d\tau \quad , \tag{2}$$

where f_0 is the central frequency, and is the window duration parameter. It is worth noting that the ST is equivalent to STFT when $f = f_0$.

Synchrosqueezing S-transform

The aim of SSST is to retrieve the ideal time-frequency representation by the instantaneous frequency estimation.

$$\hat{\omega}_s(t,f) = R\left[\frac{1}{i2\pi}\frac{\partial_t ST_s(t,f)}{ST_s(t,f)}\right] \quad , \tag{3}$$

where $!_t[¥]$ and $R[\bullet]$ represent the partial derivative and real part of a complex number, respectively.

The core idea of SSST is to rearrange the coefficients from (t,f) to $\left(t,\hat{\omega}_s(t,f)\right)$.

$$SSST_s^{\gamma}(t,\omega)=|\omega|\int_{\left|\hat{\omega}_s(t,f)\right|>\gamma} ST_s(t,f)e^{jft}\frac{\delta\left(\omega-\hat{\omega}_s(t,f)\right)}{|f|}df \quad , \qquad (4)$$

where γ denotes the threshold, and δ is the Dirac function.

Finally, the mode can be reconstructed by summing the coefficients $ST_s(t,f)$ in the vicinity of $\varphi'(t)$.

$$s(t)\approx\frac{1}{\int_{-\infty}^{+\infty}F_g(\xi-\omega_0)\frac{d\xi}{|\xi|}}\int_{|\omega-\varphi'(t)|<d}\frac{SSST_s^{\gamma}(t,\omega)}{|\omega|}d\omega \qquad (5)$$

where d is the interval parameter, and F_g is the Fourier transform of Gaussian window function g.

Demodulated synchrosqueezing S-transform

The demodulated technique mainly depends on two demodulation operators, shift demodulation operator $d_s(t)=e^{-i2\pi\int\varphi(t)dt}$ and translation demodulation operator $d_t(t,u)=e^{-i2\pi\varphi(u)t}$. So, the total demodulation operator is expressed as:

$$d(t,u)=d_s(t)\bullet d_t(t,u)=e^{-i2\pi\left(\int\varphi(t)dt-\varphi(u)t\right)} \qquad (6)$$

where $\varphi(t)$ is the instantaneous frequency ridge, u denotes the time-domain coordinate.

The product of signal $s(t)$ and $d(t,u)$ is described as:

$$s_d(t)|_{[u-\Delta,u+\Delta]}\approx s(t)\bullet d(t,u)=s(t)e^{-i2\pi\left(\int\varphi(t)dt-\varphi(u)t\right)} \quad , \quad (7)$$

where $\Delta=\omega_0 T/2|\omega|$.

The ST based on demodulated signal can be defined as:

$$ST_{s_d}(t,f)=\frac{|f|}{\sqrt{2\pi}f_0T}\int_{-\infty}^{+\infty}s_d(\tau)e^{-\left(\frac{f^2(t-\tau)^2}{2(f_0T)^2}+jf\tau\right)}d\tau \quad . \tag{8}$$

Similarly, SSST is expressed as:

$$SSST_{s_d}^{\gamma}(t,\omega)=|\omega|\int_{\left|\hat{\omega}_s(t,f)\right|>\gamma}ST_{s_d}(t,f)e^{jft}\frac{\delta\left(\omega-\hat{\omega}_{s_d}(t,f)\right)}{|f|}df \quad , \tag{9}$$

where the new instantaneous frequency is represented as:

$$\hat{\omega}_{s_d}(t,f)=\partial_t\arg\left[ST_{s_d}(t,f)\right]=R\left[\frac{1}{i2\pi}\frac{\partial_t ST_{s_d}(t,f)}{ST_{s_d}(t,f)}\right] \tag{10}$$

Finally, the mode can be approximately reconstructed by:

$$s(t)\approx\frac{e^{i2\pi\left(\int\varphi(t)dt-\varphi(u)t\right)}}{\int_{-\infty}^{+\infty}F_g(\xi-\omega_0)\frac{d\xi}{|\xi|}}\int_{|\omega-\varphi_d'(t)|<d}\frac{SSST_{s_d}^{\gamma}(t,\omega)}{|\omega|}d\omega \quad . \tag{11}$$

In addition, for a multicomponent signal, we assume that the instantaneous frequencies of the modes of the multicomponent signal are separated at each time point. Thus we can assign the respective demodulation operators to the different modes. Then, a fine TFR is achieved by combining the time-frequency distribution of each sub-domain, in which the boundary is calculated by means of average of adjacent ridges using the ridge estimation algorithm.

$$B_n(t)=\frac{\left(\varphi_n(t)+\varphi_{n+1}(t)\right)}{2},n\in[1,N-1] \quad , \tag{12}$$

where $B_0(t)=0$, and $B_N(t)$ is the half of sampling frequency. The adjacent $B_n(t)$ makes up a sub-domain for each mode to demodulate separately.

SYNTHETIC EXAMPLE

In this section, the numerical investigation is presented to demonstrate the improvements brought by the proposed DSSST in comparison with the ST and SSST on synthetic example. We apply the ST, SSST, and DSSST, respectively, on a synthetic signal that consists of three components, shown in Fig. 1, which was previously used for evaluation by Thakur et al. (2013) and Huang et al. (2015).

$$\begin{aligned} s_1(t) &= \left[2 + 0.2\cos(t)\right] \bullet \cos\left[2\pi\left(3t + 0.6\cos(t)\right)\right] \\ s_2(t) &= 0.6\left[1 + 0.3\cos(2t)\right] \bullet \exp(-t/20) \\ &\quad \bullet \cos\left[2\pi\left(5t + 0.6t^{1.8} + 0.3\sin(t)\right)\right] \\ s_3(t) &= 0.4\cos\left[2\pi(9t)\right] \\ s(t) &= s_1(t) + s_2(t) + s_3(t) + n(t) \end{aligned} \tag{13}$$

where $n(t)$ is the Gaussian noise, the sampling frequency and signal-to-noise (SNR) are 1000 Hz and 8 dB, respectively.

Figs. 2(a)-(c) show the TFR results of the synthetic signal using the ST, SSST, and DSSST. It can be seen that the ST suffers from a poor time-frequency resolution [See Fig. 2(a)]. The time-frequency energy is blurred, and it spreads out in the vicinity of the instantaneous frequencies of the signal. The operation of 'squeezing' makes the energy more concentrated on the spectrum of the SSST, which effectively improves the readability of a TFR [See Fig. 2(b)] compared with the standard ST method. However, the time-frequency curves still show the energy divergence to a certain extent, which is not conducive to instantaneous frequency estimation. By comparison, the DSSST provides a nice TFR result [See Fig. 2(c)], and the energy is perfectly concentrated than the other two methods. In order to clearly observe the performance of the above approaches, we enlarge some areas marked by the yellow and red rectangular boxes in Fig. 2, which are displayed in Figs. 3 and 4, respectively. We can clearly find the advantage of the DSSST in characterizing the non-stationary signals, which makes the time-frequency information more easily interpretable [See Figs. 3(c) and 4(c)]. For a better understanding of the improvements brought by the DSSST over other studied methods, we utilize a quantitative comparison of all these techniques in terms of energy concentration of the TFR results by employing a measure named Renyi entropy, and a lower Renyi entroy value indicates a more energy-concentrated TFR result. The Renyi entropies from the ST, SSST and DSSST methods are listed in Table 1. As can be clearly seen, the proposed DSSST has the lowest value, in other words, it achieves the optimal energy-concentrated result on the time frequency map. The Renyi entropy is defined as follows:

$$I = -\frac{1}{2}\log_2\left(\frac{\iint_{R^2}\left|TFR(t,f)\right|^3 dfdt}{\iint_{R^2}\left|TFR(t,f)\right| dfdt}\right) \tag{14}$$

where $TFR(t,f)$ is the TFR result.

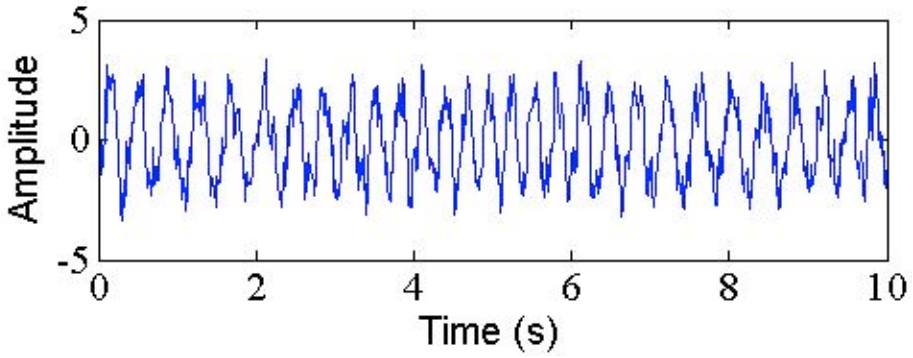

Fig. 1. A synthetic signal.

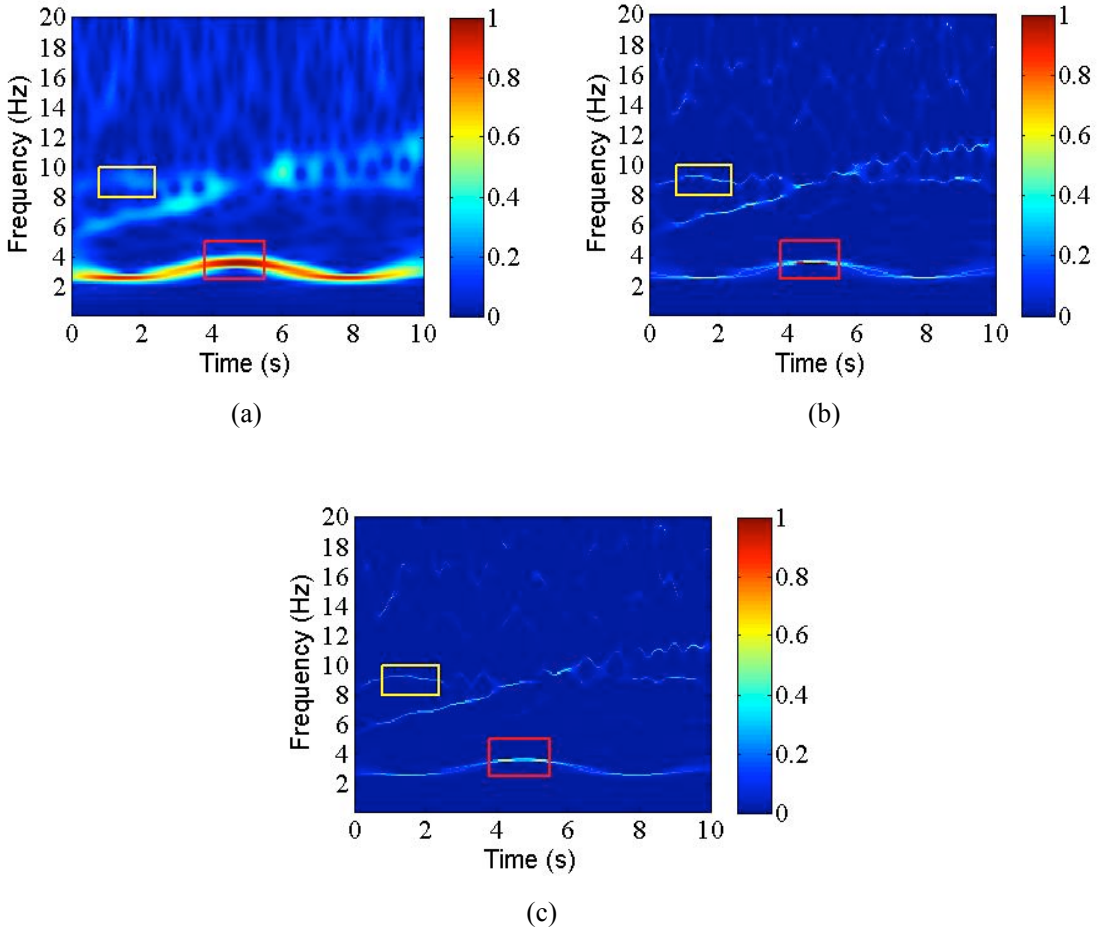

Fig. 2. Time-frequency maps obtained by ST (a), SSST (a) and DSSST (c), respectively. DSSST achieves a highly energy-concentrated TFR.

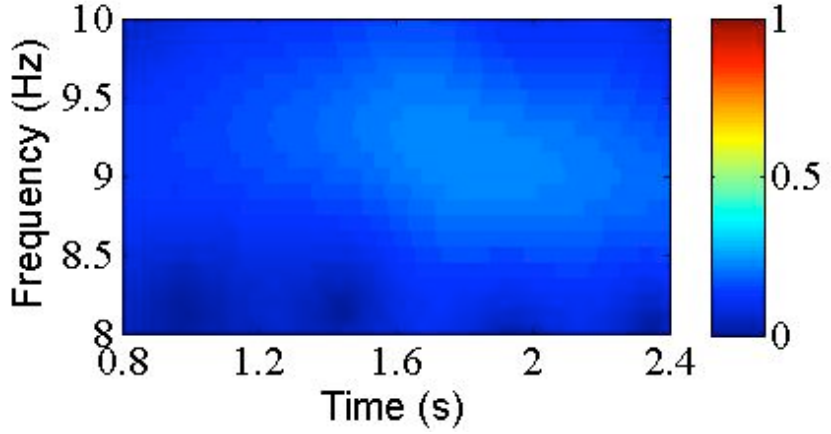

(a)

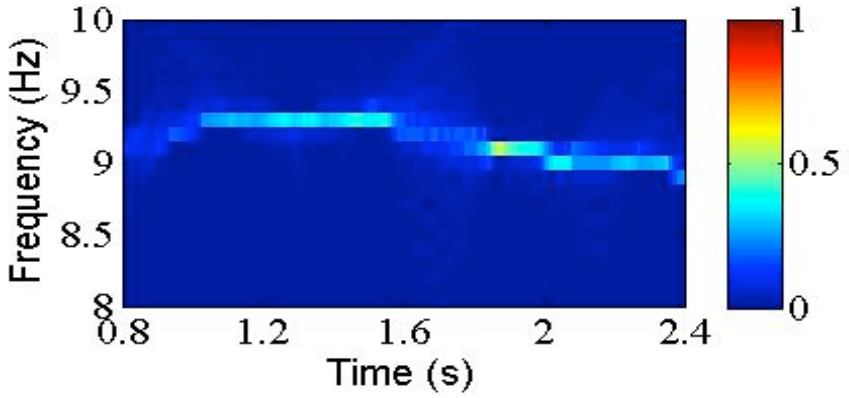

(b)

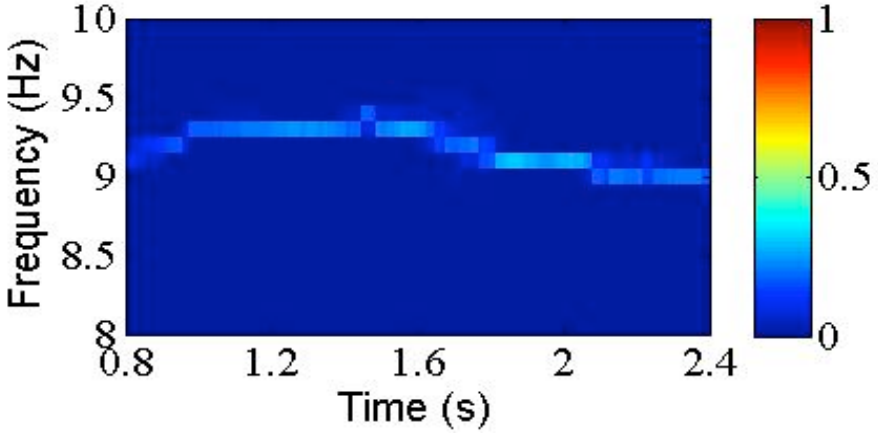

(c)

Fig. 3. Enlarged time-frequency maps from a yellow rectangular box in Fig. 2. The DSSST (c) provides a more energy-concentrated TFR result than the ST (a) and SSST (b) methods.

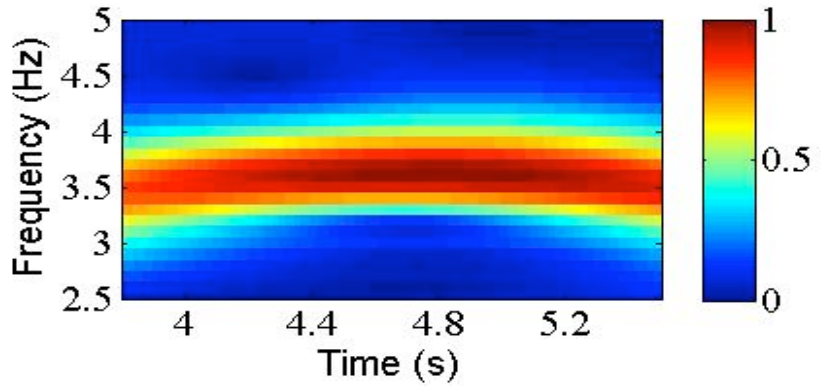

(a)

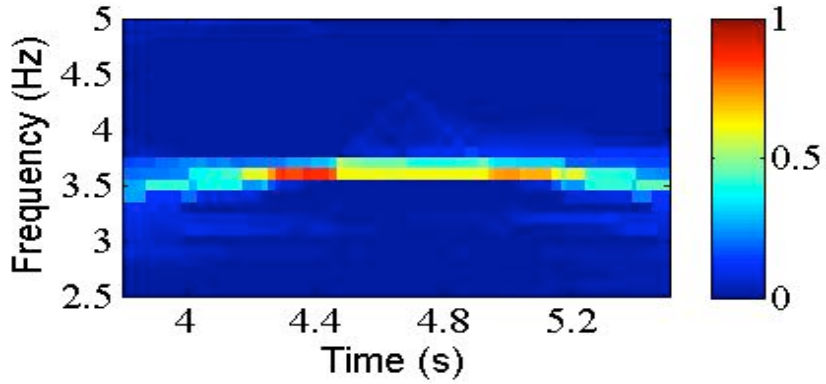

(b)

(c)

Fig. 4. Enlarged time-frequency maps from a red rectangular box in Fig. 2. The DSSST (c) has the higher time-frequency resolution compared with the ST (a) and SSST (b) methods.

Table 1. Renyi entropies of the ST, SSST and DSSST methods.

TFA	ST	SSST	DSSST
Renyi entropy	17.4192	15.5576	12.3804

FIELD EXAMPLE

We now illustrate the applicability of the proposed DSSST method in detection of hydrocarbon by using a real field data including gas-filled sand, which is composed of 60 traces, the time duration is 1s, and time sampling rate is 2 ms. The gas-filled reservoir that has been confirmed by the drilling is marked by a black arrow (Fig. 5), in which the seismic trace 20 passes through the hydrate accumulation reservoir. As shown in Fig. 6(a), the time-domain waveform of the 20th trace displays the strong amplitude around 4s. The trace 20 is processed respectively using the ST-based, SSST-based, and the DSSST-based spectral decomposition. The resulting TFR results are plotted in Figs. 6(b), 6(c) and 6(d), respectively. We can clearly see that these TFRs have the similar characteristics, for example, the strong spectral energy exists about 4s. Frequency squeezing enables better time-frequency resolution for SSST method compared with the standard ST method. In contrast with the ST and SSST results, the proposed DSSST performs obviously better, with the more interpretable instantaneous frequency due to its high resolutions both in time and frequency.

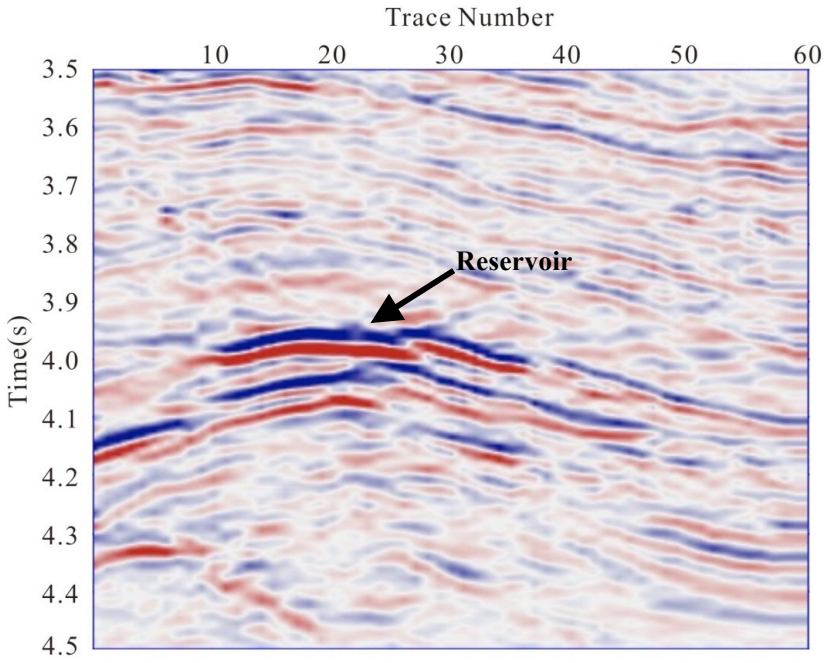

Fig. 5. The real field data.

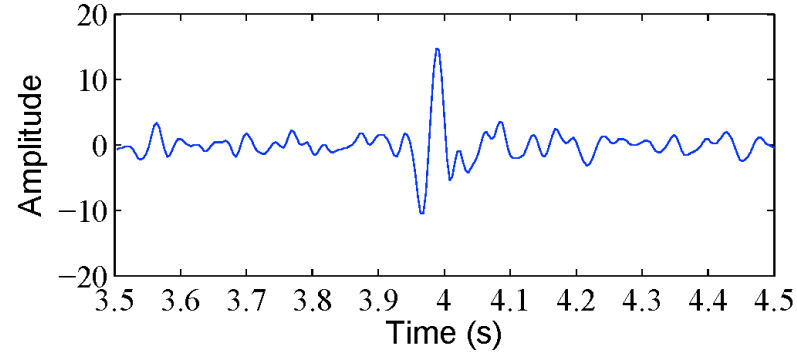

(a)

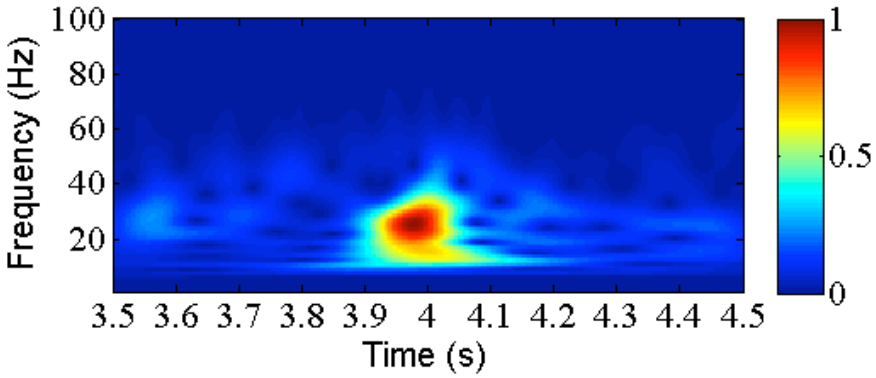

(b)

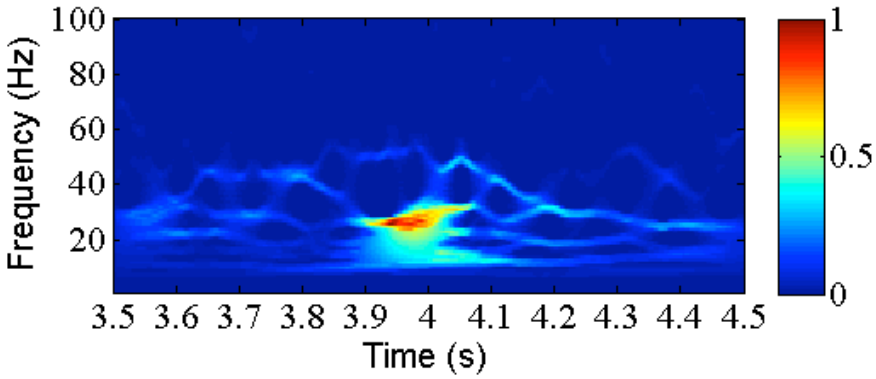

(c)

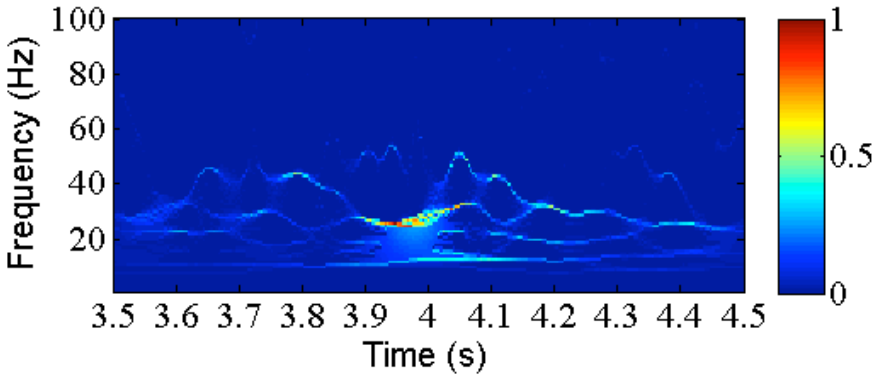

(c)

Fig. 6. Trace 20 (a) from real data in Fig. 5, and the resulting TFRs using by ST (b), SSST (c) and DSSST (d).

Figs. 7(a), 7(c) and 7(e) are respectively the 20 Hz constant-frequency slices of ST-based, SSST-based and DSSST-based spectral decomposition. Figs. 7(b), 7(d) and 7(f) are the 40 Hz constant-frequency slices of the aforementioned methods. Comparing Fig. 7(a) and 7(b), it can be found that the time-frequency energy at the location of hydrocarbon reservoir varies slightly between the 20 Hz and 40 Hz slices of ST, which makes it difficult to confirm the existence of potential hydrate accumulation. In contrast, such differences can be easily identified on the slices of SSST and DSSST. Moreover, due to the advantages of DSSST in high time-frequency resolution, the difference in energy between the two constant-frequency slices is even more prominent, which is helpful to detect the hydrate accumulation.

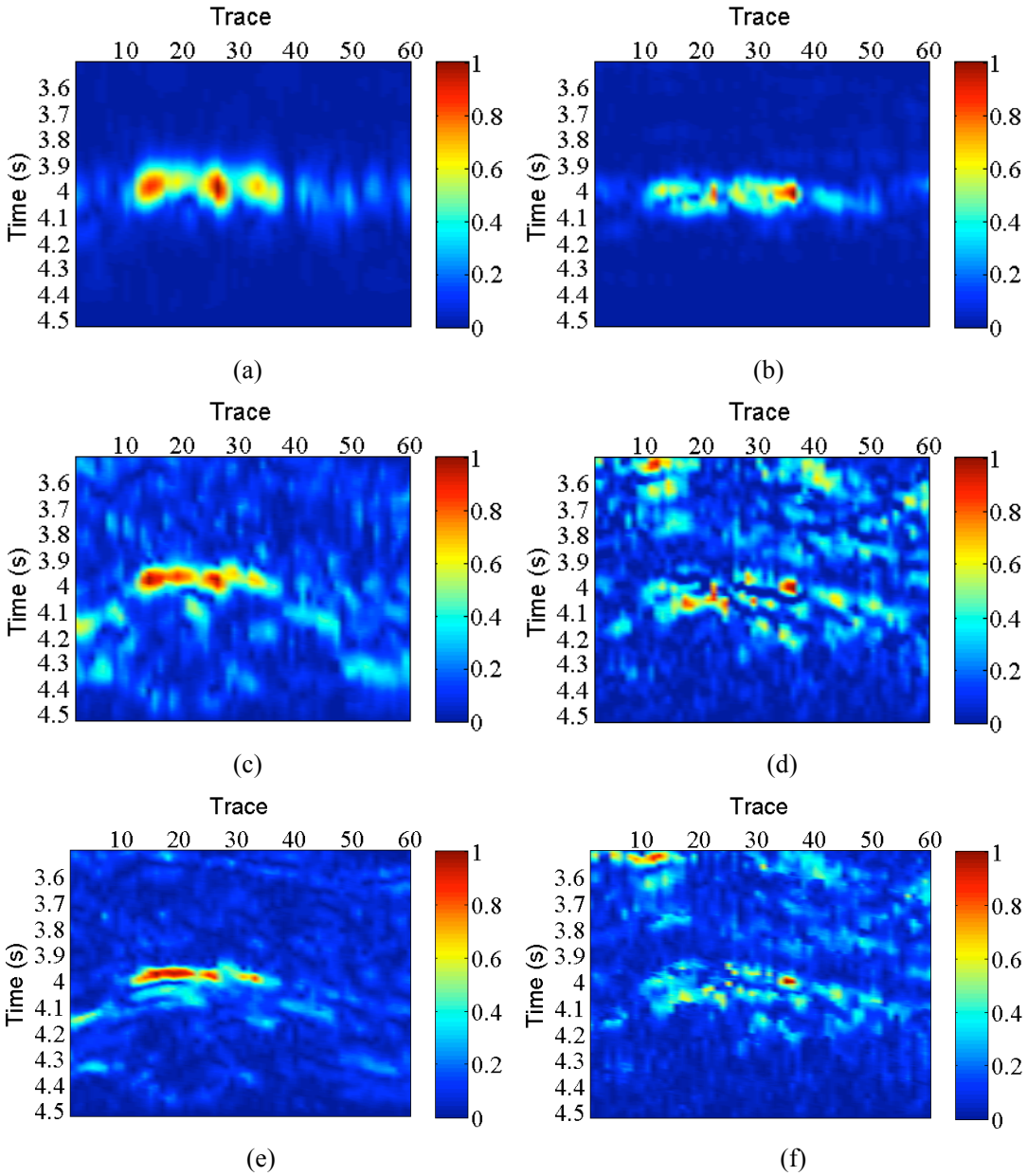

Fig. 7. Frequency slices of spectral decomposition results. (a) 20 Hz slice of ST, (b) 40 Hz slice of ST, (c) 20 Hz slice of SSST, (d) 40 Hz slice of SSST, (e) 20 Hz slice of DSSST, and (f) 40 Hz slice of DSSST. The DSSST with high time-frequency resolution is more conducive to hydrocarbon identification.

CONCLUSIONS

We propose a new technique, called DSSST, for time-frequency representation of non-stationary signals, and derive the formulas for the DSSST and its inverse transform for signal reconstruction. The DSSST introduces the demodulation technique into the SSST for more accurate instantaneous frequency estimation, thus, it effectively enhances the resolution of the time-frequency representation of signals. The result of synthetic example shows that the DSSST can accurately characterize instantaneous frequency information of seismic signal. Field data further indicates the potential of the DSSST method in detection of spectral anomalies associated with hydrocarbon reservoir, which renders this technique promising for seismic data processing and imaging. Further work should be devoted to a deeper analysis of the influence of noise on the demodulation operators.

ACKNOWLEDGEMENTS

This work was supported by the Regional Logistics Research Center Project under Grant NGY2Y-20-009.

REFERENCES

Allen, J.B., 1977. Short term spectral analysis, synthetic and modification by discrete Fourier transform. IEEE Transact. Acoust., Speech, Sign. Process., 25: 235-238.

Auger, F. and Flandrin, P., 1995. Improving the readability of time-frequency and time-scale representations by the reassignment method. IEEE Trans. Signal Process., 43(5): 1068-1089.

Castagna, J.P., Sun, S. and Siegfried, R.W., 2003. Instantaneous spectral analysis: detection of low-frequency shadows associated with hydrocarbons. The Leading Edge, 22: 120-127.

Chen, Y., Liu, T., Chen, X., Li, J. and Wang, E., 2014. Time-frequency analysis of seismic data using synchrosqueezing wavelet transform. J. Seismic Explor., 23: 303-312.

Daubechies, I., Lu, J. and Wu, H.T., 2011. Synchrosqueezed wavelet transform: An empirical mode decomposition-like tool. Appl. Comput. Harmon. Anal., 30: 243-261.

Herrera, R.H., Han, J. and van der Baan, M., 2014. Applications of the synchrosqueezing transform in seismic time-frequency analysis. Geophysics, 79(3): V55-V64.

Huang, Z., Zhang, J., Zhao, T. and Sun, Y., 2016. Synchrosqueezing S-transform and its application in seismic spectral decomposition. IEEE Transact. Geosci. Remote Sens., 54: 817-825.

Liu, N., Gao, J., Zhang, B., Wang, Q. and Jiang X., 2019. Self-adaptive generalized S-transform and its application in seismic time-frequency analysis. IEEE Transact.. Geosci. Remote Sens., 57: 7849-7859.

Liu, W., Cao, S., Liu, Y. and Chen, Y., 2016. Synchrosqueezing transform and its applications in seismic data analysis. J. Seismic Explor., 25: 27-44.

Liu, Y. and Fomel, S., 2013. Seismic data analysis using local time-frequency decomposition. Geophys. Prosp., 61: 516-525.

Sinha, S., Routh, P., Anno, P. and Castagna, J., 2005. Spectral decomposition of seismic data with continuous-wavelet transform. Geophysics, 70(6): 19-25.

Stockwell, R.G., Mansinha, L. and Lowe, R.P., 1996. Localization of the complex spectrum: the S transform. IEEE T. Signal Proces., 44(4): 998–1001.

Thakur, G., Brevdo, E., Fuckar, N.S. and Wu, H.T., 2013. The synchrosqueezing algorithm for time-varying spectral analysis: Robustness properties and new paleoclimate applications. Signal Process., 93: 1079-1094.

Thakur, G. and Wu, H.T., 2011. Synchrosqueezing-based recovery of instantaneous frequency from nonuniform samples. SIAM J. Math. Anal., 43: 2078–2095.

Wang, Q., Gao, J., Liu, N. and Jiang, X., 2018. High-resolution seismic time-frequency analysis using the synchrosqueezing generalized S-transform. IEEE Geosci. Remote Sens. Lett., 15: 374-378.

Yang, H., 2015. Synchrosqueezed wave packet transforms and diffeomorphism based spectral analysis for 1D general mode decompositions. Appl. Comput. Harmon. A., 39: 33-66.